

Molecular-state treatment of collisions between protons and  $\text{He}^+$  ions

Thomas G. Winter

*Physics Department, Pennsylvania State University, Wilkes-Barre Campus, Wilkes-Barre, Pennsylvania 18708*

Gregory J. Hatton and Neal F. Lane\*

*Physics Department, Rice University, Houston, Texas 77001*

(Received 7 March 1980)

Cross sections have been calculated for electron transfer into all states of H in collisions of protons and  $^4\text{He}^+$  ions at center-of-mass energies from 1.6 to 14 keV. Excitation of the  $2s$ ,  $2p_\sigma$ , and  $2p_\pi$  states of  $\text{He}^+$  has also been considered. The coupled-molecular-state calculations incorporate matrix elements and potential curves determined previously for up to ten molecular states  $1s\sigma$ ,  $2s\sigma$ , ...,  $3d\delta$  and up to 22 states  $1s\sigma$ ,  $2s\sigma$ , ...,  $4f\phi$ ,  $5g\sigma$ ,  $5g\pi$  in treatments with and without plane-wave translational factors, respectively. The departure from rectilinear trajectories has been estimated to affect the electron-transfer cross sections by less than 7% at energies above 1.6 keV. The present results show very good agreement with the magnitude and structure of a recent experimental cross-section curve.

## I. INTRODUCTION

Electron transfer in collisions of  $\text{He}^{++}$  ions with H atoms has been studied extensively<sup>1-6</sup> using four coupled-molecular-state approaches: the perturbed-stationary-state (pss) approach,<sup>7</sup> and modifications of it by Bates and McCarroll,<sup>8</sup> Schneiderman and Russek,<sup>9</sup> and Rankin and Thorson.<sup>10</sup> For this process, the molecular state  $2p\sigma$  is degenerate in the separated-atoms limit with the main charge-transferring states  $2p\pi$  and  $3d\sigma$ , and the  $2p\sigma$  and  $3d\sigma$  states are nearly degenerate at intermediate internuclear separations as well.<sup>1</sup> (The  $2p\sigma$  state correlates to the  $1s$  state of H, and the  $2s\sigma$ ,  $2p\pi$ , and  $3d\sigma$  states correlate to states of  $\text{He}^+$  with a principal quantum number of two in the separated-atoms limit.) It has been found that the  $2p\sigma$ ,  $2p\pi$ , and  $3d\sigma$  states are sufficient to determine the approximate value of the charge-transfer cross section; nonetheless, additional states, notably the  $3d\pi$  state, are needed for a more accurate determination of the cross section, particularly if translational factors are omitted from the treatment. The cross section has been found to be large—about  $10^{-15}$  cm<sup>2</sup> at the 8-keV peak [in the  $^4\text{He}^+-\text{H}^+$  center-of-mass (c.m.) coordinate system].<sup>3-4</sup>

The "inverse" process—charge transfer during collisions between protons and *ground-state*  $\text{He}^+$  ions—may be expected to be quite different, even though the same nuclei are involved. For the inverse process, the molecular state  $1s\sigma$  (which correlates to the initial state  $1s$  of  $\text{He}^+$ ) is highly nondegenerate with all the charge-transferring (as well as other) states at all internuclear separations. (See the correlation diagram in Fig. 1.) In contrast to the  $\text{He}^{++}-\text{H}$  process, it is not clear

at the outset for the  $\text{He}^+-\text{H}^+$  case that a few molecular states will suffice to determine the charge-transfer cross section, even if translational factors are included. In view of the nondegeneracy of

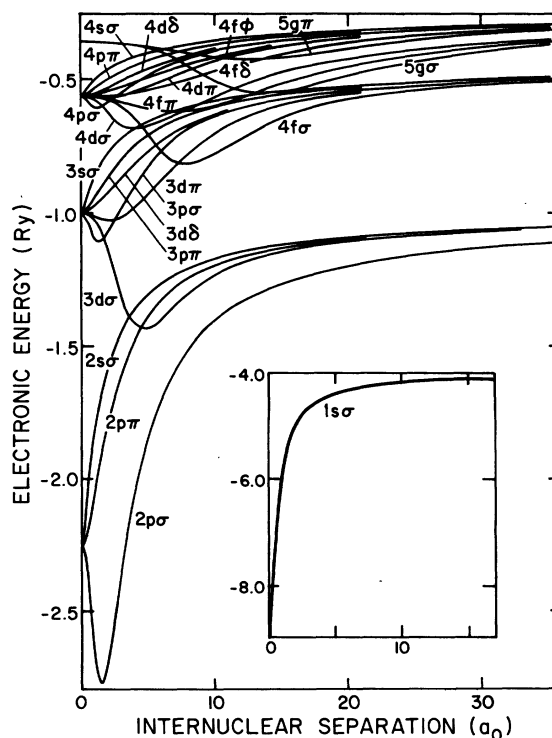


FIG. 1. Electronic energies of the lowest 20 states  $1s\sigma$ ,  $2s\sigma$ , ...,  $4f\phi$  and the  $5g\sigma$ ,  $5g\pi$  states of the  $\text{HeH}^{++}$  molecule (Ref. 4). The  $2p\sigma$ ,  $4d\sigma$ ,  $4f\pi$ , and  $5g\sigma$  states correlate to states of H with principal quantum number  $n \leq 2$  in the separated-atoms limit, and the remaining states correlate to states of  $\text{He}^+$  with  $n \leq 4$ .

the molecular energies, the cross section is expected to be small, despite several matrix elements being large (see Figs. 2-4); it is known from experiments that the cross-section maximum is only about  $3 \times 10^{-17}$  cm<sup>2</sup> at approximately 40 keV in the c.m. system,<sup>11-13</sup> and the cross section is considerably less at lower energies, where a molecular state treatment would be expected to be appropriate.

In this work, the important molecular states for the  $H^+-^4He^+$  electron-transfer process are determined using the coupled-molecular-state approaches with and without plane-wave translational factors, and the cross sections are calculated at c.m. energies from 1.6 to 14 keV. (A c.m. energy of 20 keV corresponds to a relative nuclear velocity of one atomic unit.) A comparison of cross sections is made in the region of overlap with the measurements over the energy range of 3.0 to 28.5 keV of Peart, Grey, and Dolder<sup>11</sup>; measurements have also been made from 60 to 402 keV by Mitchell, Dunn, Angel, Browning, and Gilbody<sup>12</sup> and Angel, Sewell, Dunn, and Gilbody.<sup>13</sup> Comparison is also made with the atomic-state results of Rapp<sup>14</sup> for the process of electron transfer to the *ground state* of  $He^+$  in  $He^{++}$ -H collisions. In addition, cross sections for excitation of the lower-lying states of  $He^+$  are determined.

## II. METHOD

Except for the different boundary condition, the coupled equations and their numerical solution are the same as described in Refs. 2-4 for the

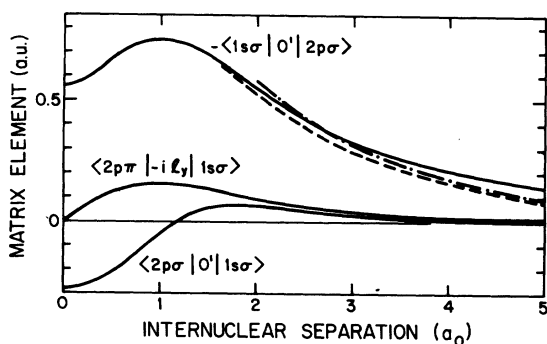


FIG. 2. Plane-wave-factor matrix elements coupling the  $1s\sigma$  state with the  $2p\sigma$  and  $2p\pi$  states. (The  $1s\sigma$ - $2p\pi$  matrix element is equivalent to the pss matrix element with origin on the He nucleus.) Only the real parts of the  $1s\sigma$ - $2p\sigma$  matrix elements are plotted: —,  $E=0$ , all  $\rho$ ; ---,  $E=4$  keV,  $\rho=0.5a_0$ ,  $z \geq 0$ ; -·-,  $E=4$  keV,  $\rho=2a_0$ ,  $z \geq 0$ . Not shown are the curves  $\langle 2p\sigma | O' | 1s\sigma \rangle$  for  $E=4$  keV, which agree closely with that shown for  $E=0$ . The operator  $O'$  is the real part of  $\exp(i\vec{v} \cdot \vec{r}) [\partial/\partial R - (\rho/zR)\ell_y]$ .

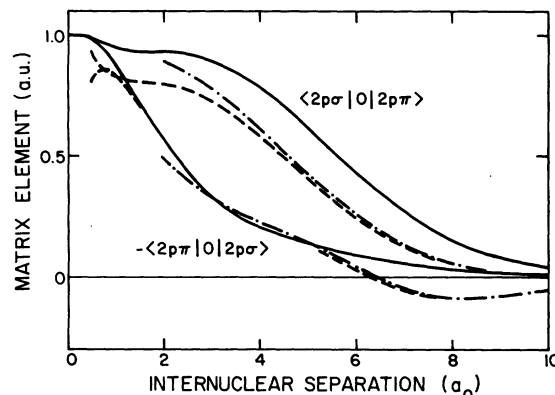


FIG. 3. Real parts of plane-wave-factor matrix elements coupling the  $2p\sigma$  and  $2p\pi$  states: —,  $E=0$ , all  $\rho$ ; ---,  $E=4$  keV,  $\rho=0.5a_0$ ,  $z \geq 0$ ; -·-,  $E=4$  keV,  $\rho=2a_0$ ,  $z \geq 0$ . The operator  $O$  is the real part of  $\exp(i\vec{v} \cdot \vec{r}) [-i\ell_y + (Rz/\rho)\partial/\partial R]$ .

$He^{++}$ -H process, and will not be repeated here. In the present case, detailed balancing has provided an additional test of numerical accuracy: Plane-wave-factor cross sections for the  $H^+-He^+$  electron-transfer process agree with values for the process of electron transfer to the ground state of  $He^+$  in  $He^{++}$ -H collisions to at least the three digits being reported here.

The pss and plane-wave-factor matrix elements appearing in the coupled equations are exactly the same as those required for the  $He^{++}$ -H process, and the numerical procedure for obtaining them was reported in Refs. 2-4. Of these matrix elements, the most important ones for the  $H^+-He^+$  electron-transfer process will be described in Sec. IIIA.

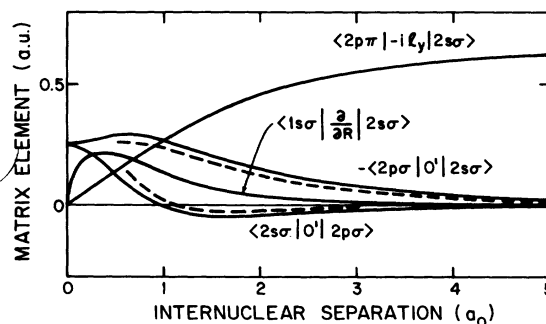


FIG. 4. Plane-wave-factor matrix elements coupling the  $2s\sigma$  state with the  $1s\sigma$ ,  $2p\sigma$ , and  $2p\pi$  states. (The  $1s\sigma$ - $2s\sigma$  and  $2p\pi$ - $2s\sigma$  matrix elements are equivalent to the pss matrix elements with origin on the He nucleus.) Only the real parts of the  $2s\sigma$ - $2p\sigma$  matrix elements are plotted: —,  $E=0$ , all  $\rho$ ; ---,  $E=4$  keV,  $\rho=0.5a_0$ ,  $z \geq 0$ . Not shown is the curve  $\langle 2p\sigma | O' | 2s\sigma \rangle$  for  $E=4$  keV,  $\rho=2a_0$ ,  $z \geq 0$ , which agrees closely with the corresponding curve for  $\rho=0.5a_0$ .

## III. RESULTS

## A. Electron transfer

Plane-wave-factor cross sections using 2–10 molecular states are presented in Table I, along with pss values for later comparison. Rectilinear trajectories have been assumed (see discussion below). Despite its small cross section (the largest value—at the highest relative velocity of 0.837 a.u.—being only  $0.07 \text{ \AA}^2$ ), the process does not involve the  $1s\sigma$  and  $2p\sigma$  states alone: The  $2p\pi$  and  $2s\sigma$  states also contribute significantly. (As shown in Fig. 1, the  $1s\sigma$  and  $2p\sigma$  states correlate, respectively, to the  $1s$  states of  $\text{He}^+$  and H.) However, the next six states collectively contribute only 5–19% over the energy range considered; and, of these, the  $3d\sigma$  state, essential for describing the  $\text{He}^{++}\text{-H}(1s)$  process,<sup>1-4</sup> now contributes at most 6% up to 6 keV and only 15% even at the highest energy of 14 keV.

To better illustrate details of the dynamics of the collision, including the roles of various states, the probability times impact parameter  $\rho P(\rho)$  has been plotted versus impact parameter  $\rho$  in Figs. 5 and 6 for representative c.m. energies of 1.6 and 14 keV. It is seen that only small impact parameters  $\rho \leq 3 a_0$  contribute significantly to the integrated cross section; indeed, there are no peaks in  $\rho P(\rho)$  beyond  $\rho = 1.4 a_0$ . The  $2p\pi$  state is very important, and, at the smaller impact parameters, the  $2s\sigma$  state is also important. Since the shape of  $\rho P(\rho)$  is roughly independent of the size of basis if at least the four states  $1s\sigma$ ,  $2p\sigma$ ,  $2p\pi$ , and  $2s\sigma$  are included, the role of various states in the evolution of the collision in time  $t$  can be examined to some extent by plotting  $P(\rho, z)$  versus  $z = vt$  at the most important peaks of  $\rho P(\rho)$ . (The states are, however, not orthogonal for finite  $|z|$ .) In Figs. 7–9 these curves are illustrated for an energy

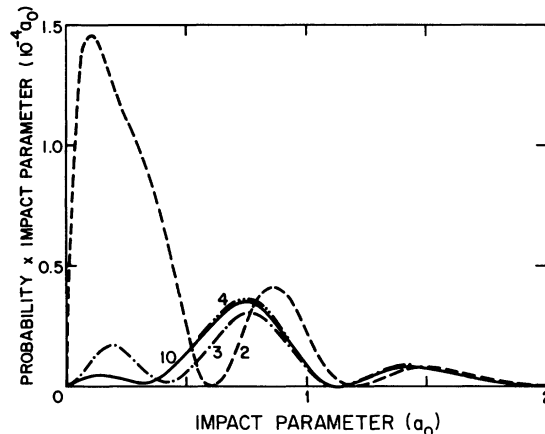


FIG. 5. Probability times impact parameter for electron transfer in 1.6-keV  $\text{H}^+ - {}^4\text{He}^+$  collisions. Results are shown for the plane-wave-factor bases of 2, 3, 4, and 10 states indicated in the text and Table I.

$E = 1.6 \text{ keV}$ ,  $\rho = 0.7$ , and  $1.4 a_0$ , and  $E = 14 \text{ keV}$ ,  $\rho = 1.4 a_0$ , respectively. The important collision dynamics are confined to the region  $|z| \leq 5 a_0$ , with the dominant interactions occurring in the region  $|z| \leq 2.5 a_0$ . At the lower energy (particularly at the larger impact parameter), the three-state ( $1s\sigma$ ,  $2p\sigma$ ,  $2p\pi$ ) and four-state ( $1s\sigma$ ,  $2p\sigma$ ,  $2p\pi$ ,  $2s\sigma$ ) curves look like the two-state ( $1s\sigma$ ,  $2p\sigma$ ) one and share the near symmetry about  $z = 0$ . However, the electron-transfer amplitudes are sufficiently small asymptotically so that the probabilities are sensitive to small changes in the shapes of the curves at small  $|z|$ . [The need for four states to describe the electron-transfer process persists down to at least 0.6 keV, where  $P(\rho) < 10^{-7}$ .]

Finally, the confinement of the collision to a small range in  $\rho$  and  $|z|$  is consistent with the

TABLE I. Total cross sections (in units of  $\text{\AA}^2$ ) for electron transfer into all states of H in collisions between  $\text{H}^+$  and  ${}^4\text{He}^+(1s)$  ions. The coupled-state<sup>a</sup> calculations were performed both with and without plane-wave translational factors, with the origin placed on the helium nucleus in the latter case. Rectilinear nuclear trajectories have been assumed.

c.m. energy (keV)	Number of states with plane-wave factors					Number of states without plane-wave factors	
	2	3	4	5	10	5	10
1.6	11.3(-5) <sup>b</sup>	3.22(-5)	3.38(-5)	3.41(-5)	3.23(-5)	2.94(-5)	2.93(-5)
3	9.40(-4)	9.34(-4)	7.84(-4)	7.43(-4)	7.28(-4)	5.77(-4)	5.98(-4)
4	3.27(-3)	3.52(-3)	2.56(-3)	2.46(-3)	2.28(-3)	1.79(-3)	1.83(-3)
6	15.9(-3)	8.82(-3)	6.75(-3)	6.50(-3)	5.63(-3)	3.78(-3)	4.34(-3)
8	3.39(-2)	1.32(-2)	1.36(-2)	1.22(-2)	1.24(-2)	0.780(-2)	1.02(-2)
14	6.96(-2)	6.45(-2)	7.55(-2)	6.45(-2)	7.16(-2)	3.65(-2)	5.76(-2)

<sup>a</sup> The two states  $1s\sigma$ ,  $2p\sigma$ ; the three, four, and five states obtained by successively adding  $2p\pi$ ,  $2s\sigma$ , and  $3d\sigma$  to  $1s\sigma$ ,  $2p\sigma$ ; and the ten states  $1s\sigma$ ,  $2s\sigma$ , . . . ,  $3d\delta$ .

<sup>b</sup> The number in parentheses denotes the power of ten by which the preceding number is to be multiplied.

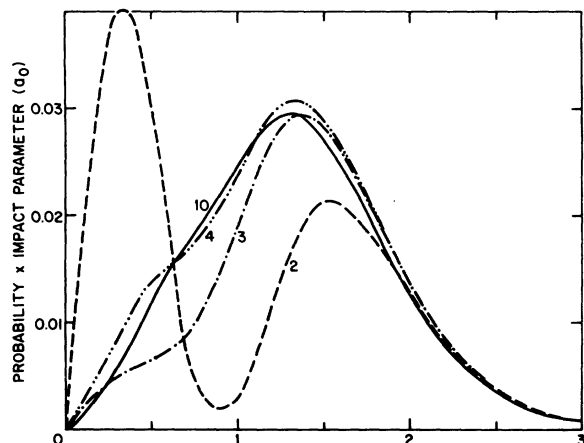


FIG. 6. Probability times impact parameter for electron transfer in 14-keV  $H^+-^4He^+$  collisions.

$1s\sigma$ ,  $2p\sigma$ ,  $2p\pi$ , and  $2s\sigma$  matrix elements plotted in Figs. 2-4; these matrix elements (after being multiplied, where appropriate, by the angular velocity  $v\rho/R^2$ ) are of short range. This behavior undoubtedly reflects the compactness of the  $1s\sigma$  wave function, strongly centered on the He nucleus for all  $R$ , and its tendency to couple with the other comparatively compact functions—i.e., those for the  $2p\sigma$ ,  $2p\pi$ , and  $2s\sigma$  states. Being nearly degenerate for small internuclear separations, these three states are more likely to mix among themselves than with more highly excited states. The nondegenerate  $3d\sigma$  state has little chance to be populated by the  $2p\sigma$  state, since the  $1s\sigma$ - $2p\sigma$  coupling occurs only at small  $R$ . Thus, in contrast to the  $He^{++}$ -H electron-transfer process,<sup>3-4</sup> here the  $3d\sigma$  and  $3d\pi$  states play minor roles. The large magnitude of the  $2p\sigma$ - $2p\pi$  matrix elements

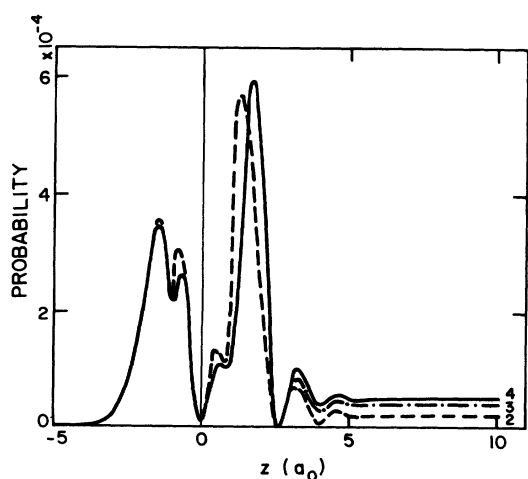


FIG. 7. Probability versus  $z$  for electron transfer in 1.6-keV  $H^+-^4He^+$  collisions at an impact parameter of  $0.7a_0$ .

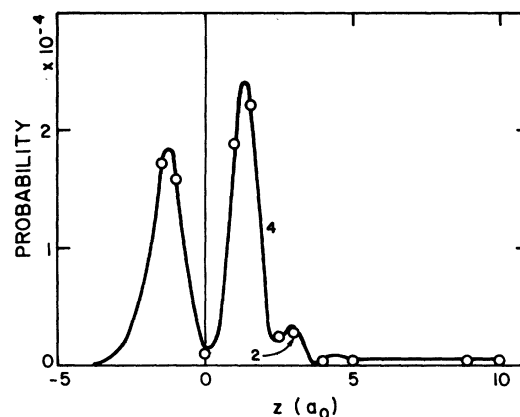


FIG. 8. Probability versus  $z$  for electron transfer in 1.6-keV  $H^+-^4He^+$  collisions at an impact parameter of  $1.4a_0$ . Only a few two-state points are shown, since they generally lie on the four-state curve (solid line).

implies that there is interference among the  $1s\sigma$ ,  $2p\sigma$ , and  $2p\pi$  amplitudes; the  $2p\pi$  state does not merely drain flux from the  $1s\sigma$  state. Indeed, the three-state-cross-section curves (not shown) versus  $E$  for electron transfer and  $2p_1(He^+)$  excitation have different shapes, as would not have been expected if the amplitudes had added incoherently.

Also shown in Table I are electron-transfer cross sections obtained without plane-wave factors, with fixed origin placed on the helium nucleus. These five- and ten-state pss values differ by at most 13% for  $E \leq 6$  keV, comparable to the differences when plane-wave factors are included; at higher energies ( $\leq 14$  keV), the differences of up to 37% are greater than the corresponding differences when plane-wave factors are included,

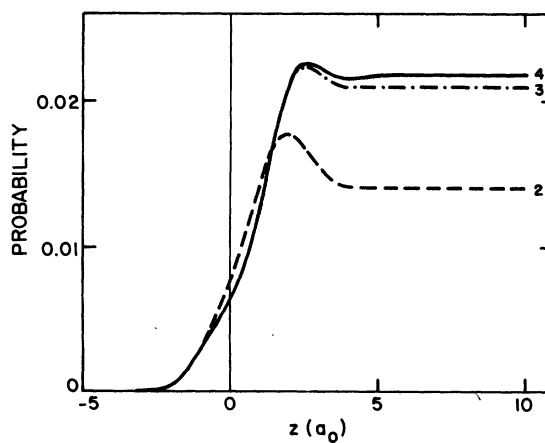


FIG. 9. Probability versus  $z$  for electron transfer in 14-keV  $H^+-^4He^+$  collisions at an impact parameter of  $1.4a_0$ .

reflecting the desirability of translational factors when the relative nuclear velocity approaches the orbital electronic velocity. The ten-state pss cross section is  $(20 \pm 3)\%$  below the corresponding value with plane-wave factors, except at the lowest energy where it is below by 9%. Since the convergence in going from five- to ten-state plane-wave-factor cross sections is generally better than that for the two corresponding pss cases, it is reasonable to suppose that the differences between ten-state pss and plane-wave-factor cross sections mainly reflect the need for more states in the pss calculation. By recalculating pss values of  $\rho P(\rho)$  using 22 states ( $1s\sigma, 2s\sigma, \dots, 4f\varphi, 5g\sigma, 5g\pi$ ) for  $E = 4, 8, \text{ and } 14$  keV at the more important peak impact parameters, this assumption has been largely confirmed: The new values differ from the ten-state plane-wave-factor values by at most 13%, except at the highest energy where the difference is 17.5%. The convergence of pss values to plane-wave-factor values at higher energies appears to be more rapid in the present case than in the case of the  $\text{He}^{2+}\text{-H}$  process studied previously (with an origin chosen to be on H in the latter case.) The present pss calculation provides an estimate of the most likely additional contributors to the plane-wave-factor cross section, those states ( $4d\sigma, 4f\pi, 5g\sigma$ ) which correlate to the lowest excited states of H in the separated-atoms limit. For capture into all states, it is found that the contribution from these three basis states is less than 4% at peak impact parameters. (Up to 20% of the charge-transfer flux goes into these excited states, but the ground state is depleted.)

The effect of the departure from rectilinear trajectories on the electron-transfer cross section has been estimated using a different simple trajectory (a Coulombic trajectory) to decrease from 7% at 1.6 keV to 1% at 8 keV. (See Table II.)

The present cross sections for electron transfer into all states are compared with the correspond-

TABLE II. Total cross sections (in units of  $\text{\AA}^2$ ) for electron transfer into all states of H in collisions between  $\text{H}^+$  and  ${}^4\text{He}^+(1s)$  ions with rectilinear and Coulombic trajectories. The calculations were performed using five states ( $1s\sigma, 2p\sigma, 2p\pi, 2s\sigma, 3d\sigma$ ) without plane-wave factors, and with the origin placed on the helium nucleus.

c.m. energy (keV)	Trajectory	
	Rectilinear	Coulombic
1.6	2.94(-5)	2.74(-5)
4	1.79(-3)	1.72(-3)
8	0.780(-2)	0.770(-2)

ing experimental values of Peart, Grey, and Dolder<sup>11</sup> in Fig. 10. The present values are the ten-state, plane-wave-factor results, believed to be the best of the theoretical values reported in Table I. The experimental error bars shown are the sums of the estimated random errors (90% confidence limits) and the estimated bound on systematic errors (7%).<sup>11</sup> The values of Peart *et al.* tie in well with the measured values of Angel, Sewell, Dunn, and Gilbody (not shown) at higher energies.<sup>13</sup> It is seen that there is very good agreement in the overlapping range of c.m. energies from 3 to 14 keV. The results agree within the error bars at the lower and higher energies; the slopes and shapes of the curves—especially the dip at the intermediate energies—agree well, and the theoretical values lie above the upper limits of the estimated error bars by only 13–14% at the intermediate energies of 4 and 6 keV. While the effect of additional higher lying states on the plane-wave-factor cross section is difficult to estimate, it is to be noted in Table I that the addition of states to form the ten-state basis results in gradual lowering of the cross section at the intermediate energies, bringing it closer to the experimental result; furthermore, the effect of the last block of five states is only 8–15%.

Also shown in Fig. 10 are the coupled-atomic-state results of Rapp<sup>14</sup> for the process of electron transfer to the *ground state* in  $\text{He}^{2+}\text{-H}$  collisions. By detailed balancing these results should be equivalent to those for capture into the ground state in  $\text{H}^+\text{-He}^+$  collisions. Neither the atomic-state results nor the present results take into account capture into excited states of H; however, in the present case, an estimate of these excited-

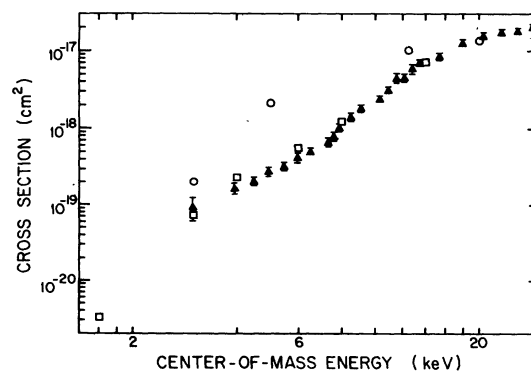


FIG. 10. Total cross sections for electron transfer in  $\text{H}^+\text{-}{}^4\text{He}^+$  collisions. Theoretical results:  $\square$ , the present ten-molecular-state results with plane-wave factors;  $\circ$ , the eleven-atomic-state results of Rapp (Ref. 14). The experimental data:  $\blacktriangle$ , Peart, Grey, and Dolder (Ref. 11).

TABLE III. Total cross sections (in units of  $\text{\AA}^2$ ) for excitation of the  $2s$ ,  $2p_0$ , and  $2p_1$  states of  $\text{He}^+$  in collisions between  $\text{H}^+$  and  $^4\text{He}^+(1s)$  ions. The coupled-molecular-state<sup>a</sup> calculations were performed both with plane-wave-translational factors (the MPW approximation) and without them (the pss approximation), with the origin placed on the helium nucleus in the latter case. Rectilinear nuclear trajectories have been assumed.

c.m. energy (keV)	Number of basis states	Excited state, approximation					
		$2s$ , MPW	$2s$ , pss	$2p_0$ , MPW	$2p_0$ , pss	$2p_1$ , MPW	$2p_1$ , pss
1.6	5	6.51(-6)	8.77(-6)	5.62(-6)	6.12(-6)	7.95(-6)	6.77(-6)
1.6	10	6.40(-6)	7.38(-6)	4.71(-6)	5.57(-6)	7.40(-6)	6.77(-6)
3	5	4.58(-5)	6.99(-5)	9.38(-5)	11.37(-5)	1.48(-4)	1.23(-4)
3	10	4.95(-5)	5.85(-5)	7.43(-5)	9.71(-5)	1.45(-4)	1.26(-4)
4	5	3.08(-4)	3.49(-4)	4.06(-4)	4.53(-4)	4.20(-4)	3.12(-4)
4	10	3.30(-4)	2.78(-4)	2.66(-4)	4.09(-4)	4.01(-4)	3.28(-4)
6	5	2.52(-3)	3.22(-3)	6.28(-4)	7.31(-4)	1.61(-3)	1.01(-3)
6	10	2.82(-3)	2.62(-3)	3.78(-4)	7.46(-4)	1.43(-3)	1.09(-3)
8	5	4.70(-3)	6.84(-3)	2.78(-3)	2.89(-3)	3.64(-3)	2.12(-3)
8	10	5.39(-3)	5.77(-3)	1.79(-3)	2.78(-3)	3.05(-3)	2.23(-3)
14	5	2.60(-2)	4.45(-2)	1.23(-2)	1.98(-2)	1.31(-2)	0.680(-2)
14	10	2.66(-2)	3.71(-2)	0.840(-2)	1.74(-2)	1.12(-2)	0.641(-2)

<sup>a</sup>The five states  $1s\sigma$ ,  $2p\sigma$ ,  $2p\pi$ ,  $2s\sigma$ ,  $3d\sigma$ , and the ten states  $1s\sigma$ ,  $2s\sigma$ , . . . ,  $3d\delta$ .

state contributions has been noted to be small. The atomic-state results disagree with the molecular-state results and experimental results at all energies.

#### B. Excitation of the $\text{He}^+$ ion

Plane-wave-factor and pss cross sections for excitation of the  $2s$ ,  $2p_0$ , and  $2p_1$  states of the  $\text{He}^+$  ion are presented in Table III. These cross sections have been calculated using the same five and ten molecular-basis states as were used in the calculation of electron-transfer cross sections. Trajectories have again been assumed to be rectilinear; this assumption will be discussed below. Not shown are two-state ( $1s\sigma$ ,  $2p\pi$ ) and three-state ( $1s\sigma$ ,  $2p\pi$ ,  $2p\sigma$ ) values of the  $2p_1$  cross section; these cross sections differ from one another by up to an order of magnitude, illustrating that in considering excitation it is not always safe to neglect charge-transfer states (e.g., the  $2p\sigma$  state here). For excitation of the  $2s$  or  $2p_1$  states, the five- and ten-state, plane-wave-factor cross sections agree to within 16%, agreement comparable to that found for electron transfer. For the excitation of the  $2p_0$  state, however, the addition of five states changes the cross section by up to 40%. Also shown in Table III are pss cross sections using an origin on the helium nucleus; for the process of exciting the helium ion, there are clear physical grounds for choosing this origin. For the excitation of the  $2s$  state, the (10-state) pss and plane-wave-factor cross sections differ by at most 17% except at the highest energy of 14 keV, where the difference amounts to 33%.

For the excitation of the  $2p_0$  and  $2p_1$  states at the higher energies ( $\geq 6$  keV), the differences between the pss and plane-wave-factor cross sections are large (as much as a factor of 2). The nonsphericity of the states, and the smaller size of the cross sections, are both reasons for expecting these cross sections to be more sensitive to the inclusion of plane-wave factors than the electron-transfer cross sections.

The effect of the departure from rectilinear trajectories on the excitation cross sections has been estimated using a Coulombic trajectory (see Table IV). At c.m. energies of at least 4 keV, the effect is small, and comparable to that for electron transfer (see Table II). However, at

TABLE IV. Total cross sections (in units of  $\text{\AA}^2$ ) for excitation of the  $2s$ ,  $2p_0$ , and  $2p_1$  states of  $\text{He}^+$  in collisions between  $\text{H}^+$  and  $^4\text{He}^+(1s)$  ions with rectilinear and Coulombic trajectories. The calculations were performed using five states ( $1s\sigma$ ,  $2p\sigma$ ,  $2p\pi$ ,  $2s\sigma$ ,  $3d\sigma$ ) without plane-wave factors, and with the origin placed on the helium nucleus.

c.m. energy (keV)	State	Trajectory	
		Rectilinear	Coulombic
1.6	$2s$	8.77(-6)	7.0(-6)
1.6	$2p_0$	6.12(-6)	3.8(-6)
1.6	$2p_1$	6.77(-6)	7.50(-6)
4	$2s$	3.49(-6)	3.31(-4)
4	$2p_0$	4.53(-4)	4.28(-4)
4	$2p_1$	3.12(-4)	3.14(-4)
8	$2s$	6.84(-3)	6.78(-3)
8	$2p_0$	2.89(-3)	2.82(-3)
8	$2p_1$	2.12(-3)	2.13(-3)

the lowest energy (1.6 keV), the effect is larger (particularly for the  $2s$  and  $2p_0$  states) than it is for electron transfer; at this energy the excitation probabilities  $P(\rho)$  are strongly affected by the choice of trajectory for  $\rho \lesssim 0.5 a_0$  (not shown).

## ACKNOWLEDGMENTS

This work was supported in part by the Department of Energy, Office of Basic Energy Sciences, and the Robert A. Welch Foundation.

---

\*Present address: The National Science Foundation, Washington, D. C. 20550.

<sup>1</sup>R. D. Placentini and A. Salin, *J. Phys. B* 7, 1666 (1974); 9, 563 (1976); 10, 1515 (1977).

<sup>2</sup>T. G. Winter and N. F. Lane, *Phys. Rev. A* 17, 66 (1978).

<sup>3</sup>G. J. Hatton, N. F. Lane, and T. G. Winter, *J. Phys. B* 12, L571 (1979).

<sup>4</sup>T. G. Winter and G. J. Hatton, *Phys. Rev. A* 21, 793 (1980).

<sup>5</sup>J. Vaaben and K. Taulberg, *Abstracts of Papers, Eleventh International Conference on the Physics of Electronic and Atomic Collisions*, Kyoto, Japan, 1979 (The Society for Atomic Collision Research, Kyoto, 1979), p. 566.

<sup>6</sup>M. Kimura and W. R. Thorson, *Bull. Am. Phys. Soc.*

24, 1188 (1979).

<sup>7</sup>D. R. Bates, H. S. W. Massey, and A. L. Stewart, *Proc. R. Soc. London Ser. A* 216, 437 (1953).

<sup>8</sup>D. R. Bates and R. McCarroll, *Proc. R. Soc. London Ser. A* 247, 175 (1958).

<sup>9</sup>S. B. Schneiderman and A. Russek, *Phys. Rev.* 181, 311 (1969).

<sup>10</sup>J. Rankin and W. R. Thorson, *Phys. Rev. A* 18, 1990 (1978).

<sup>11</sup>B. Peart, R. Grey, and K. T. Dolder, *J. Phys. B* 10, 2675 (1977).

<sup>12</sup>J. B. A. Mitchell, K. F. Dunn, G. C. Angel, R. Brown-  
ing, and H. B. Gilbody, *J. Phys. B* 10, 1897 (1977).

<sup>13</sup>G. C. Angel, E. C. Sewell, K. F. Dunn, and H. B. Gil-  
body, *J. Phys. B* 11, L297 (1978).

<sup>14</sup>D. Rapp, *J. Chem. Phys.* 61, 3777 (1974).